Hydrogen Production Hot Paper

Deutsche Ausgabe: DOI: 10.1002/ange.201501971
Internationale Ausgabe: DOI: 10.1002/anie.201501971

Micromotor-Based Energy Generation**

*Virendra V. Singh, Fernando Soto, Kevin Kaufmann, and Joseph Wang**

Abstract: *A micromotor-based strategy for energy generation, utilizing the conversion of liquid-phase hydrogen to usable hydrogen gas (H_2), is described. The new motion-based H_2-generation concept relies on the movement of Pt-black/Ti Janus microparticle motors in a solution of sodium borohydride ($NaBH_4$) fuel. This is the first report of using $NaBH_4$ for powering micromotors. The autonomous motion of these catalytic micromotors, as well as their bubble generation, leads to enhanced mixing and transport of $NaBH_4$ towards the Pt-black catalytic surface (compared to static microparticles or films), and hence to a substantially faster rate of H_2 production. The practical utility of these micromotors is illustrated by powering a hydrogen–oxygen fuel cell car by an on-board motion-based hydrogen and oxygen generation. The new micromotor approach paves the way for the development of efficient on-site energy generation for powering external devices or meeting growing demands on the energy grid.*

Supplying the world's increasing demand for portable and practical energy generation are fundamental challenges of the 21st century.[1] Hydrogen (H_2) offers considerable promise as an alternative energy source owing to its low environmental impact, light weight, and high energy density.[2] Various technologies are available for H_2 storage, such as high-pressure cylinders, liquefaction, and reformation from hydrocarbons. However, owing to various drawbacks of these technologies, on-board H_2 storage is still a major obstacle for practical use.[2] Liquid-phase chemical hydrogen-storage materials, such as $NaBH_4$, N_2H_4, MgH_2, $LiBH_4$, or H_3NBH_3, have received substantial interest as H_2 storage media owing to their ability to generate high-purity H_2.[3–9] Among these, sodium borohydride ($NaBH_4$) is an attractive candidate offering several advantages, including high hydrogen density, non-flammable, controllable hydrogen-generation rate, moderate operation temperature, stability in alkaline solutions, and nontoxic hydrolysis by-products.[10]

Noble metals exhibit the fastest known conversion rates of $NaBH_4$ and are thus widely used for H_2 generation.[11–13] In most studies, these catalysts have been used as a film, embedded in a support material, or as metal nanoparticles. However, these approaches have certain limitations owing to inherent problems, such as surface passivation (deactivation of catalyst by the by-product, $NaBO_2$), heterogeneous distribution of fuel, and aggregation and destabilization of metal nanoparticles.[11,14,15]

Herein we describe a new self-propelled catalytic micromotor-based strategy for rapid energy production from liquid fuels and demonstrate its capability for powering external devices. Recent advances in the field of micromotors[16] have led to their growing use for accelerating chemical reaction rates compared to static particles, owing to efficient fluid mixing that arises from the self-propulsion of micromotors.[17] This mixing has been shown to be extremely effective in accelerating target-receptor interactions,[18] bio-detection,[19] and detoxification and decontamination processes.[17b,20]

The new "on-the-move" H_2-generation concept represents the first demonstration of using self-propelled micromotors for energy applications. Such motor-based H_2 generation exploits the continuous movement of Pt-black/Ti Janus microparticle motors in $NaBH_4$ fuel solution. This operation is also the first example of using $NaBH_4$ as a fuel for micromotor propulsion and involves a surfactant-free solution. The autonomous motion of catalytic micromotors in the $NaBH_4$ fuel solution and their effective bubble generation provide a favorable hydrodynamic environment that leads to dramatically enhanced fuel supply to the catalytic surface, and thus to rapid H_2 generation, compared with that obtained from a static catalyst. Static catalysts commonly suffer from blocking of the catalyst sites by adhered H_2 bubbles and precipitation of reaction by-products.[11,14,15]

Finally, we demonstrate the first use of catalytic micromotors to power a hydrogen–oxygen fuel cell model car by on-board micromotor-based production of H_2 and oxygen (O_2), using $NaBH_4$ and H_2O_2, respectively, as liquid fuel storage media for the anode and cathode. Such generation of energetically rich gas products was thus integrated with a fuel cell for converting chemical energy into electrical energy. The micromotor-based approach could lead to efficient on-site H_2 generation, address challenges associated with H_2 transportation and storage, and open new energy-generation opportunities towards an environmentally friendly energy future.

A schematic of the micromotor-based H_2 production is given in Figure 1 A. This new strategy for H_2 production relies on the generation of high-density microbubble tails from autonomously moving Pt-black/Ti Janus particle micromotors, through the catalytic decomposition of the $NaBH_4$ fuel at the Pt-black surface. The fabrication of Janus micromotors, consisting of a Ti layer coating half of the Pt-black microparticles, is detailed in the Experimental Section. The SEM image of Figure 1 B illustrates the morphology of the Janus micromotor (ca.20 μm) with a titanium film coating the Pt-

[*] Dr. V. V. Singh,[+] F. Soto,[+] K. Kaufmann, Prof. J. Wang
Department of Nanoengineering
University of California, San Diego
La Jolla, CA 92093 (USA)
E-mail: josephwang@ucsd.edu

[+] These authors contributed equally to this work.

[**] This project received support from the Defense Threat Reduction Agency-Joint Science and Technology Office for Chemical and Biological Defense (Grant no. HDTRA1-13-1-0002). F.S. is a UC MEXUS-CONACYT Doctoral Fellow.

Supporting information for this article is available on the WWW under http://dx.doi.org/10.1002/anie.201501971.

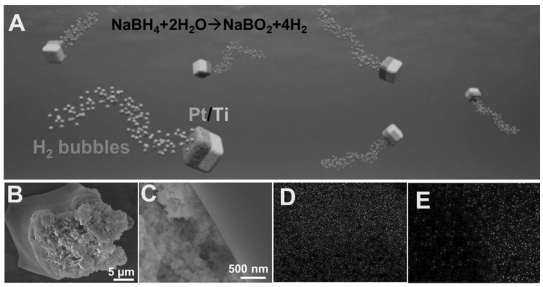

Figure 1. A) Schematic representation of the self-propulsion of Janus micromotors by the production of H_2 microbubbles in the presence of $NaBH_4$. SEM images of B) the Pt-black/Ti particle, C) Pt-black/Ti interface; EDX images showing the D) Pt-black and E) titanium surfaces.

black. This and additional SEM and energy dispersive X-ray spectroscopy (EDX) data (Figure 1 B–E) indicate that the microparticles have a distinct binary structure with a smooth Ti layer coating half of the highly porous Pt-black particle. The porous Pt-black provides a high catalytic surface area responsible for effective bubble evolution in the presence of $NaBH_4$.

The effective propulsion of the new motors reflects the continuous thrust of H_2 bubbles generated by the spontaneous catalytic reaction with the $NaBH_4$ fuel and leads to a motor speed of 250 $\mu m s^{-1}$ and an enhanced mass-fluid transport, as expected from previous reports.[17a] Figure 2 A shows microscope images illustrating the movement of the Pt-black/Ti micromotors in $NaBH_4$ solution at 150 ms intervals (taken from Supporting Information Video S1). A long high-density tail of H_2 microbubbles is generated and ejected from the microporous Pt-black surface. Similarly, Figure 2 B demonstrates the simultaneous movement of multiple motors and their ability to generate H_2 microbubbles. As illustrated below, optimizing the micromotor density can be used to increase the H_2 production rate. As expected, the speed of the

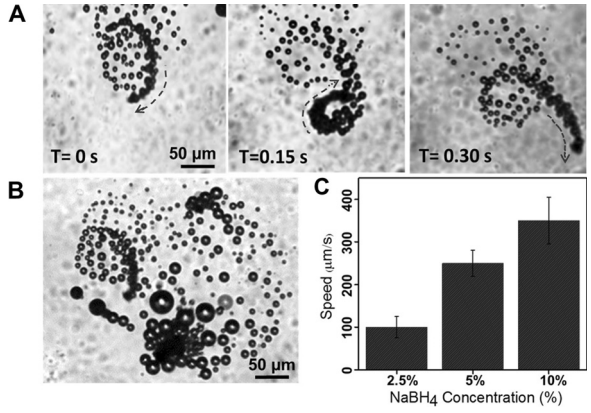

Figure 2. Effective propulsion of Pt-black/Ti micromotors and generation of H_2 microbubbles. A) Time-lapse images over 0.15 s, taken from Video S1 in the Supporting Information, illustrating the motion of micromotors; B) image, taken from Video S2, illustrating the motion of multiple micromotors; C) Motor speed dependence on fuel concentration. Reaction conditions (A) and (B): 5% $NaBH_4$/2% NaOH solution.

Pt-black/Ti micromotors is strongly dependent on the $NaBH_4$ fuel, increasing from 100 to 250 to 350 $\mu m s^{-1}$ using 2.5%, 5%, and 10% fuel concentrations, respectively (Figure 2 C).

To further investigate and optimize the efficient H_2 production of the $NaBH_4$-powered micromotors, we examined the influence of the amount of micromotors, fuel, and NaOH concentrations by measuring the evolved H_2 gas per unit time (using the pneumatic trough shown in Figure S1). The solution pH value was carefully monitored, since $NaBH_4$ can undergo self-hydrolysis.[21] It was found that the H_2-generation rate decreased dramatically upon increasing the NaOH concentration, as expected from earlier studies;[22] therefore, only 2% NaOH was used to inhibit the self-hydrolysis reaction of $NaBH_4$. The amount of Pt-black/Ti micromotors was varied from 0.1 mg to 1.5 mg in a 500 μL aqueous solution containing 5 wt% $NaBH_4$ and 2 wt% NaOH (Figure 3 B). The liberated H_2 was measured with

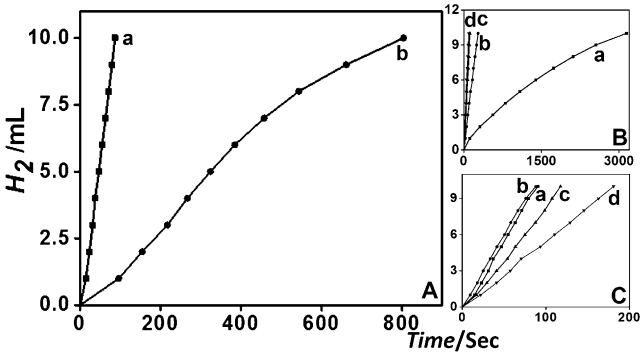

Figure 3. Micromotor-based H_2 generation from hydrolysis of $NaBH_4$: A) H_2 generation rate in the presence of self-propelled Janus micromotors (a) and static micromotors (b); reaction conditions: 500 μL solution containing 0.5 mg respective micromotors and 5% $NaBH_4$/2% NaOH. B) H_2 generation in the presence of different amounts of micromotors: a) 0.1 mg, b) 0.5 mg, c) 1.0 mg, and d) 1.5 mg, using 5% fuel. C) H_2 generation in the presence of different fuel concentrations: a) 5%, b) 10%, c) 15%, and d) 20%, using 0.5 mg micromotors.

respect to time by measuring the volume of water displaced in the gas collection chamber (Figure S1). As indicated in Figure 3 B, the rate of H_2 generation increases rapidly with the motor density up to 0.5 mg and then nearly levels off. Figure 3 C shows the influence of the fuel concentration and illustrates that 5% $NaBH_4$ is the optimum level for motor-based H_2 generation. These studies indicate that the generation rate is affected more by fuel concentration than micromotor density. This data is consistent with related literature,[23] including optimal H_2 generation between 5–10% $NaBH_4$. The H_2 production rate decreases using lower $NaBH_4$ concentrations because of limited fuel supply; alternatively, higher fuel concentrations lead to diminished production rate because of increased surface passivation by excess $NaBO_2$.[11,14,15]

To determine the effect of the surface area of Pt-black on the H_2 generation rate, a comparative study was made using smooth sputtered Pt Janus particles (described in the Experimental Section). A fixed amount (0.5 mg) of these particles,

was placed in the reaction vessel containing 500 μL aqueous solution of 5% $NaBH_4$ with 2% NaOH. Although the amount of micromotors used was identical to that in Figure 3 (involving porous motor surfaces), the data in Figure S2 indicates that the smooth catalytic surfaces result in a 90-times slower H_2 generation rate and no motion was observed compared to the Pt-black/Ti micromotors. This finding reflects the large catalytic surface area of Pt-black which provides an efficient H_2 generation rate by fast diffusion and interaction within the reaction medium.[24]

Currently used catalysts for liquid-based energy conversion are static thin films or static particles. Static Pt-black particles were used for control experiments by adding a thin Ni layer to the Ti surface to hold them stationary in the reaction vessel using a magnet. Comparison of the micromotors to their static catalytic counterpart was carried out using the same pneumatic trough. The results, displayed in Figure 3A, indicate that micromotors offer a dramatically increased H_2 production rate compared to static Pt-black/Ti/Ni (generating 10 mL H_2 within 87 s vs. 804 s, respectively). The substantial (ca. 9.2-times) difference in the H_2 generation rate is attributed to the induced motion, which leads to enhanced mixing and convection and thus to a steady supply of fuel at the catalytic surface, compared to the diffusion limited process of the static particles. The autonomous motion of the catalyst also minimizes blocking of the catalytic sites by the $NaBO_2$ reaction by-product.[25] It was also found that the H_2 gas bubbles generated adhere to the static catalyst and detach very slowly, hence hindering the continuous fuel supply to the catalyst surface.

Finally, the practical utility of the hydrogen-generating micromotors was demonstrated by powering a hydrogen–oxygen fuel cell model car by on-board co-generation of H_2 and O_2. While the use of H_2 for powering fuel cells has significant advantages, its storage and transportation remain major challenges. The present approach is based on the micromotor-driven catalytic generation of H_2 and O_2, from $NaBH_4$ and H_2O_2 fuels, respectively, in separate compartments using the same novel Pt-black/Ti micromotors.

Figure 4A shows the actual car powered by the micromotor generated energetically rich gases and outlines the different components needed to power the engine and LEDs. Figure 4B shows a schematic representation of the reactions involved in the micromotor-driven production of both gaseous fuels and simultaneous conversion to electrical energy by a proton-exchange membrane (PEM) hydrogen–oxygen fuel cell. The fuel for the PEM is H_2 and the charge carrier is the H^+ (proton). At the anode, the H_2 generated by the micromotors is split into H^+ ions and electrons. At the cathode, O_2 produced by the micromotors combines with the electrons and H^+ to produce water. The H^+ ions permeate across the electrolyte to the cathode while the electrons flow through an external circuit and produce electric power. Video S3 illustrates the ability of these motors to co-generate sufficient H_2 and O_2, even at low motor density, to power the model car. Further details of the fabrication and function of the micromotor-driven vehicle are provided in the Experimental Section. Such on-board gas generation supplies fuel directly to the two electrodes and requires no gas storage.

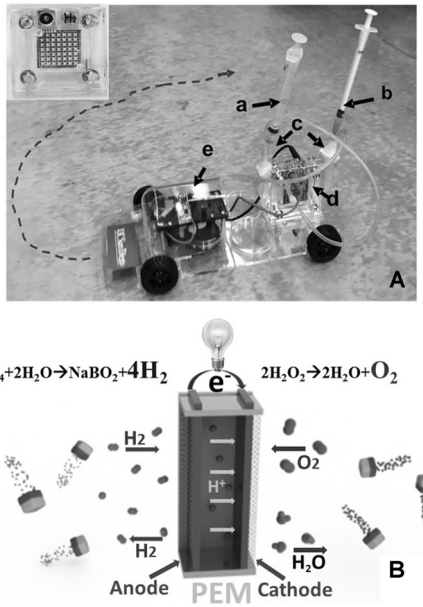

Figure 4. A) The micromotor-driven fuel-cell car based on "on-board" production of H_2 and O_2 using $NaBH_4$ and H_2O_2, respectively: a) $NaBH_4$ reservoir, b) H_2O_2 reservoir, c) dry micromotor powder, d) motor-based hydrogen–oxygen fuel cell (as shown in inset), and e) electric motor; B) schematic representation of the hydrogen–oxygen PEM fuel cell based on co-generation of H_2 and O_2 from the micromotor-driven catalysis of $NaBH_4$ and H_2O_2, respectively.

In conclusion, we present the first use of self-propelled catalytic micromotors for mobile H_2 generation and the first demonstration of micromotors propelled by $NaBH_4$ fuel. The micromotor-based generation of energetically rich gas products was used for powering a small car prototype with a fuel-cell involving in situ H_2 and O_2 generation. The autonomous motion of the Pt-black microparticles in the presence of $NaBH_4$ leads to enhanced fluid transport and to a greatly increased H_2 generation rate compared to that possible with static catalytic particles. The present findings demonstrate the importance of micromotor movement for rapid and efficient H_2 production. This approach represents a departure from traditional H_2 production methods, could address challenges associated with H_2 storage, transportation and delivery, and opens the door to on-site energy generation systems with low environmental impact.

Experimental Section

Reagents and Apparatus: $NaBH_4$ (Sigma–Aldrich, USA), NaOH (Sigma–Aldrich, USA), Pt-black particle (< 20 μm, Sigma–Aldrich, USA), Syringe (BD, USA), PEM fuel cell car (Horizon, Singapore).

Preparation of the Micromotors: The catalytic Pt-black/Ti Janus micromotors were fabricated using Pt-black particles as the base. Pt-black particles were dispersed in isopropanol (100 μL) and then spread onto the glass slides and dried under room temperature. The microparticles were coated with a thin, inert Ti layer using a Denton Discovery 18 sputter system. The deposition was performed at room temperature with a DC power of 200 W and an Ar pressure of 2.5 mTorr for 60 s. To obtain a uniform Janus half-shell coating, rotation was turned off and the sample slides were set up at an angle parallel to the Ti target. For the static micromotors (control experi-

ments), the Ti layer (20 nm) was deposited by e-beam and then subsequently a Ni layer of 50 nm was added. For comparison to smooth Pt Janus particles, silica particles were half-coated with a smooth Pt layer using a Denton Discovery 18 sputter system. The deposition was performed at room temperature with a DC power of 200 W and an Ar pressure of 2.5 mTorr for 90 s.

Propulsion of Janus Micromotors: The propulsion of Pt-black micromotors was performed in the $NaBH_4$ fuel solution. An inverted optical microscope (Nikon Instrument Inc. Ti-S/L100), coupled with a 20× and 10× objective, a Photometrics QuantEM 512/SC camera (Roper Scientific) and a MetaMorph 7.6 software (Molecular Devices) were used for capturing videos at a frame rate of 30 frames per s. The speed of the micromotors was tracked using a MetaMorph tracking module and the results were statistically analyzed using Origin software.

Measurement of Hydrogen Gas Evolution: To measure the evolved hydrogen gas by micromotors and static particles, a pneumatic trough consisting of a reaction vessel, a 10 mL top fitted syringe sealed with wax, and an inverted trap filled with and immersed in water was used (Figure S1). The micromotors were kept in a sealed Eppendorf tube and the syringe was used to inject the alkaline $NaBH_4$ inside the Eppendorf. A piece of plastic tubing was placed in a hole in the stopper at the top of the Eppendorf. This tubing fed the generated gas into the graduated cylinder filled with water and by measuring the height of displaced water, the volume of generated H_2 gas was measured. The gas collection chamber was calibrated to within 0.1 mL by a graduated cylinder, graduated beaker, and calibrated pipette.

PEM model car: A modified Horizon brand proton exchange membrane fuel cell car (model FCJJ-II) was use for demonstrating the utility of the research. The operation is based on on-board generation of energy, where micromotors were stored in two separate Eppendorf tubes mounted on the model car, with a syringe used to inject $NaBH_4$ and H_2O_2 into their respective compartments, to produce H_2 and O_2 gas bubbles. A piece of plastic tubing was placed in a hole in the stopper at the top of the Eppendorf tubes which fed the generated gas into the PEM.

Keywords: sustainable chemistry · fuel cell · hydrogen · micromotors · sodium borohydride

How to cite: *Angew. Chem. Int. Ed.* **2015**, *54*, 6896–6899
Angew. Chem. **2015**, *127*, 7000–7003

[1] Z. L. Wang, W. Wu, *Angew. Chem. Int. Ed.* **2012**, *51*, 11700; *Angew. Chem.* **2012**, *124*, 11868.
[2] a) L. Schlapbach, A. Zuttel, *Nature* **2001**, *414*, 353; b) A. C. Dillon, K. M. Jones, T. A. Bekkedahl, C. H. Kiang, D. S. Bethune, M. J. Heben, *Nature* **1997**, *386*, 377; c) C. Liu, Y. Y. Fan, M. Liu, H. T. Cong, H. M. Cheng, M. S. Dresselhaus, *Science* **1999**, *286*, 1127.
[3] H. L. Jiang, S. K. Singh, J. M. Yan, X. B. Zhang, Q. Xu, *ChemSusChem* **2010**, *3*, 541.
[4] A. M. Ozerova, V. I. Simagina, O. V. Komova, O. V. Netskina, G. V. Odegova, O. A. Bulavchenko, N. A. Rudina, *J. Alloys Compd.* **2012**, *513*, 266.
[5] M. H. Grosjean, L. Roué, *J. Alloys Compd.* **2006**, *416*, 296.
[6] P. Wang, X. D. Kang, *Dalton Trans.* **2008**, 5400.
[7] H. Zhang, Y. S. Loo, H. Geerlings, J. Lin, W. S. Chin, *Int. J. Hydrogen Energy* **2010**, *35*, 176.
[8] D. Xu, H. Wang, Q. Guo, S. Ji, *Fuel Process. Technol.* **2011**, *92*, 1606.
[9] a) J. M. Yan, X. B. Zhang, H. Shioyama, Q. Xu, *J. Power Sources* **2010**, *195*, 1091; b) T. B. Marder, *Angew. Chem. Int. Ed.* **2007**, *46*, 8116; *Angew. Chem.* **2007**, *119*, 8262; c) N. Patel, R. Fernandes, A. Santini, A. Miotello, *Int. J. Hydrogen Energy* **2012**, *37*, 2007; d) F. H. Stephens, V. Pons, R. T. Baker, *Dalton Trans.* **2007**, 2613.
[10] H. B. Dai, Y. Liang, P. Wang, H. M. Cheng, *J. Power Sources* **2008**, *177*, 17.
[11] Y. Kojima, K. Suzuki, K. Fukumoto, M. Sasaki, T. Yamamoto, Y. Kawai, H. Hayashi, *Int. J. Hydrogen Energy* **2002**, *27*, 1029.
[12] a) M. Zahmakiran, S. Ozkar, *Langmuir* **2009**, *25*, 2667; b) Z. T. Xia, S. H. Chan, *J. Power Sources* **2005**, *152*, 46; c) J. S. Zhang, W. N. Delgass, T. S. Fisher, J. P. Gore, *J. Power Sources* **2007**, *164*, 772.
[13] a) C. W. Yoon, L. G. Sneddon, *J. Am. Chem. Soc.* **2006**, *128*, 13992; b) Q. Zhang, G. Smith, Y. Wu, R. Mohring, *Int. J. Hydrogen Energy* **2006**, *31*, 961.
[14] B. H. Liu, Z. Peng Li, S. Suda, *J. Alloys Compd.* **2009**, *468*, 493.
[15] J. Cheng, C. Xiang, Y. Zoun, H. Chu, S. Qiu, H. Zhang, L. Sunnn, F. Xu, *Ceram. Int.* **2015**, *41*, 899.
[16] a) J. Wang, *Nanomachines: Fundamentals and Applications*, Wiley, Hoboken, **2013**; b) W. F. Paxton, S. Sundararajan, T. E. Mallouk, A. Sen, *Angew. Chem. Int. Ed.* **2006**, *45*, 5420; *Angew. Chem.* **2006**, *118*, 5546; c) S. Sánchez, L. Soler, J. Katuri, *Angew. Chem. Int. Ed.* **2015**, *54*, 1414; *Angew. Chem.* **2015**, *127*, 1432; d) J. G. S. Moo, M. Pumera, *Chem. Eur. J.* **2015**, *21*, 58; e) M. Guix, C. C. Mayorga-Martinez, A. Merkoçi, *Chem. Rev.* **2014**, *114*, 6285.
[17] a) J. Orozco, B. Jurado-Sanchez, G. Wagner, W. Gao, R. Vazquez-Duhalt, S. Sattayasamitsathit, M. L. Galarnyk, A. Cortés, D. Saintillan, J. Wang, *Langmuir* **2014**, *30*, 5082; b) J. Orozco, G. Cheng, D. Vilela, S. Sattayasamitsathit, R. Vazquez-Duhalt, G. Valdes-Ramirez, O. S. Pak, A. Escarpa, C. Kan, J. Wang, *Angew. Chem. Int. Ed.* **2013**, *52*, 13276; *Angew. Chem.* **2013**, *125*, 13518.
[18] a) J. Orozco, S. Campuzano, D. Kagan, M. Zhou, W. Gao, J. Wang, *Anal. Chem.* **2011**, *83*, 7962; b) D. Kagan, S. Campuzano, S. Balasubramanian, F. Kuralay, G. U. Flechsig, J. Wang, *Nano Lett.* **2011**, *11*, 2083; c) S. Balasubramanian, D. Kagan, C. M. Jack Hu, S. Campuzano, M. J. Lobo-Castanon, N. Lim, D. Y. Kang, M. Zimmerman, L. Zhang, J. Wang, *Angew. Chem. Int. Ed.* **2011**, *50*, 4161; *Angew. Chem.* **2011**, *123*, 4247.
[19] a) E. Morales-Narváez, M. Guix, M. Medina-Sánchez, C. C. Mayorga-Martinez, A. Merkoçi, *Small* **2014**, *10*, 2542; b) S. Campuzano, D. Kagan, J. Orozco, J. Wang, *Analyst* **2011**, *136*, 4621; c) X. Yu, Y. Li, Y. J. Wu, H. Ju, *Anal. Chem.* **2014**, *86*, 4501; d) M. García, J. Orozco, M. Guix, W. Gao, S. Sattayasamitsathit, A. Escarpa, J. Wang, *Nanoscale* **2013**, *5*, 1325.
[20] a) W. Gao, J. Wang, *ACS Nano* **2014**, *8*, 3170; b) L. Soler, S. Sanchez, *Nanoscale* **2014**, *6*, 7175;; c) L. Soler, V. Magdanz, V. M. Fomin, S. Sanchez, O. G. Schmidt, *ACS Nano* **2013**, *7*, 9611; d) J. Li, V. V. Singh, S. Sattayasamitsathit, J. Orozco, K. Kaufmann, R. Dong, W. Gao, B. Jurado-Sanchez, Y. Fedorak, J. Wang, *ACS Nano* **2014**, *8*, 11118; e) V. V. Singh, B. Jurado-Sánchez, S. Sattayasamitsathit, J. Orozco, J. Li, M. Galarnyk, Y. Fedorak J. Wang, *Adv. Funct. Mater.* **2015**, *25*, 2147; f) S. Sattayasamitsathit, K. Kaufmann, M. Galarnyk, R. Vazquez-Duhalt, J. Wang, *RSC Adv.* **2014**, *4*, 27565; g) B. Jurado-Sánchez, S. Sattayasamitsathit, W. Gao, L. Santos, Y. Fedorak, V. V. Singh, J. Orozco, M. Galarnyk, J. Wang, *Small* **2015**, *11*, 499.
[21] a) M. Yadav, Q. Xu, *Energy Environ. Sci.* **2012**, *5*, 9698; b) D. Xu, H. Zhang, W. Ye, *Catal. Commun.* **2007**, *8*, 1767.
[22] a) S. C. Amendola, S. L. Sharp-Goldman, M. S. Janjua, N. C. Spencer, M. T. Kelly, P. J. Petillo, *Int. J. Hydrogen Energy* **2000**, *25*, 969; b) Z. Liu, B. Guo, S. H. Chan, E. H. Tang, L. Hong, *J. Power Sources* **2008**, *176*, 306.
[23] W. Ye, H. Zhang, D. Xu, L. Ma, B. Yi, *J. Power Sources* **2007**, *164*, 544.
[24] N. Sahiner, F. Seven, *Fuel Process. Technol.* **2015**, *132*, 1.
[25] P. R. Gogate, A. B. Pandit, *Adv. Environ. Res.* **2004**, *8*, 553.

Received: March 2, 2015
Published online: April 23, 2015

